Effect of a combination of *Atractylodes macrocephala* extract with strychnine on the TLR4/NF-κB/NLRP3 pathway in MH7A cells

YIJING GAO, DAN XIN, XIAO-DONG LIANG and YINGXUE TANG

College of Traditional Chinese Medicine, Shandong University of Traditional Chinese Medicine, Jinan, Shandong 250355, P.R. China

Received September 12, 2022; Accepted December 6, 2022

DOI: 10.3892/etm.2023.11791

Abstract. Rheumatoid arthritis (RA) is now widely recognized as a chronic systemic inflammatory autoimmune disease characterized by swelling, pain and stiffness, which are often disabling. Although the number of drugs available for the treatment of RA has increased in recent years, they are generally expensive, leave patients prone to relapse and can result in severe effects when discontinued. Thus, there is a need for an inexpensive drug with fewer side effects that can be adhered to relieve pain and slow down the progression of the disease. Strychnine, a traditional Chinese medicine, was often used in ancient times to treat swollen and painful joints; however, because of its somewhat toxic nature, it is often combined with *Atractylodes macrocephala* to reduce its toxicity for safer therapeutic action. The present study performed high-performance liquid chromatography (HPLC)-tandem mass spectrometry (MS/MS) analysis to confirm whether the use of strychnine with *Atractylodes macrocephala* had the effect of reducing strychnine content. MH7A cells were induced using IL-1β to study the effect of strychnine with *Atractylodes macrocephala* on the Toll-like receptor 4 (TLR4)/NF-κB/NLR family pyrin domain-containing 3 (NLRP3) pathway in order to verify its role in the treatment of RA. The results indicated that the combined application of HPLC-MS/MS strychnine and *Atractylodes macrocephala* had a reducing effect on the strychnine content. From the subsequent experimental results, it can be inferred that Strychnine combined with *Atractylodes macrocephala* extract could promote the apoptosis of synovial cells, and could inhibit the expression levels of TLR4, NF-κB and NLRP3 in the cells as well as reducing the MH7A-positive cells. The expression levels of TLR4, IκB kinase β, NF-κB and NLRP3 were significantly reduced after treatment with each administration group, resulting in a decrease in the phosphorylation levels of TLR4 and NF-κB, indicating that the combination potently inhibited their phosphorylation. The combination of strychnine and atractylenolide II was also revealed to be the main active ingredient in the treatment of RA.

Correspondence to: Professor Xiao-Dong Liang or Professor Yingxue Tang, College of Traditional Chinese Medicine, Shandong University of Traditional Chinese Medicine, 4655 University Road, Changqing, Jinan, Shandong 250355, P.R. China
E-mail: doctorlxd@sina.cn
E-mail: doctoryxt@sina.cn

Key words: rheumatoid arthritis, strychnine, brucine, *Atractylodes macrocephala*, MH7A cells, Toll-like receptor 4, NF-κB, NLR family pyrin domain-containing 3

Introduction

Rheumatoid arthritis (RA) is a chronic, systemic autoimmune disease (1-3), which is characterized by pain and swelling, stiffness and deformity of the joints, and this can lead to disability in severe cases. *In vivo*, it manifests as persistent synovitis, systemic inflammation and the generation of autoantibodies (4), elevated levels of pro-inflammatory cytokines and inflammatory mediators such as interleukins IL-1β, IL-6, IL-8, TNF-α, chemokines and interferons from synovial tissue (5-7), leading to the development of disease and even accumulation of peripheral organs (8). The impaired joint function and dysfunction induced by RA limit a patient's ability to move freely and seriously affects daily life, resulting in increased psychological stress, reduced quality of life and a heavy financial burden (9,10).

Research into the pathogenesis of RA is not yet fully understood, but it is generally accepted that its development is associated with genetics, environmental factors and immune dysregulation (11). Associated pathogenic mechanisms include an imbalance between Th1 and Th2 cells and Th17/Treg cells, leading to an inflammatory response in the synovium and activation of synovial fibroblasts, leading to the development of RA (12,13). Fibroblastic synovial cells (FLS), a common type of cell found in synovial joints, serves an important role in the development of RA and the over-proliferation of FLS has been reported to be a significant factor in joint damage in RA (14,15). MH7A cells are an RA synovial fibroblast cell line and an established *in vitro* cell model for the study of RA (16). An early step in the development of RA is the activation of synovial fibroblasts, which causes local autoimmune cells to infiltrate the synovial tissues in response and promote the release of pro-inflammatory cytokines leading to ongoing synovial inflammation. Toll-like receptor (TLR), an important pattern recognition receptor mediating

natural immunity, mediates signaling pathways that play an important role in the development of inflammation (17). During the development of inflammation, NLR family pyrin domain-containing 3 (NLRP3), NF-κB and other inflammatory pathways are activated as a result of the excitement of TLR4 on the cell membrane (18). TLR4 primarily plays a role in triggering an immune response and phagocytosis of bacteria when substances that cause activation of MH7A cells bind to TLR4 and activate NF-κB phosphorylation and thus translocation to the nucleus, thereby initiating NLRP3 inflammatory vesicles (19). Inflammasomes were first proposed by Tschopp in 2002 (20), and among the several subtypes of inflammasomes, the NLPR3 inflammasome is one of the most extensively studied; a multi-class protein complex thought to be widely involved in the body's inflammatory and immune responses, it is widely present in immune cells, including granulocytes, antigen-presenting cells (APCs), macrophages, T and B lymphocytes (21) and in inflammatory vesicles, by activating Caspase-1, IL-β and IL-8 and initiating an inflammatory response (22,23).

Strychnine, the dried mature seeds of *Strychnos nurvomica L.* (family, Strychnosaceae), has a long history of use in Chinese medicine and has been widely used in China for swelling and pain in joints (24,25). In modern times, strychnine is also widely used in Chinese medicine to treat diseases such as cancer and orthopedic and inflammatory conditions (26-28). The primary pharmacological component of strychnine are alkaloids, which account for 1.5-5% of the total chemical composition (29), with strychnine being the most abundant and potent component (30). Alkaloid constituents in strychnine have strong and long-lasting analgesic effects. Brucine is not only a medicinal component of strychnine but is also a toxic constituent. It has toxic effects on the nervous, immune, urinary and digestive systems (31-34). These toxic effects are the main reason that the widespread use of strychnine in clinical practice is limited (35-37).

It has been demonstrated that strychnine significantly inhibits TNF-induced proliferation of HFLS-RA through activation of the JNK signaling pathway (25). The mechanism of action of strychnine and *Tripterygium wilfordii* in the treatment of RA is through the blocking of the angiogenic mediator cascade by targeting multiple interactions (38). Research has confirmed that Atractylodes macrocephala extract has an antagonistic effect on the intestinal absorption of strychnine (39). A study has confirmed the antagonistic effect of *Atractylodes macrocephala* extract on the intestinal absorption of stilbene (39). The above studies show strychnine's potential in the clinical treatment of RA.

Methotrexate is an anti-folate oncology drug but has been revealed to treat RA as early as 1951 (40). It also has a specific role; as a first-line anti-rheumatic drug, it modulates the function of the inflammatory cells involved in rheumatoid arthritis (41). Because it is highly efficacious and well-tolerated, is beneficial in the vast majority of patients and, if used early in life, will achieve the same results as other biological agents (42). Therefore, the present study selected methotrexate as a control drug.

In the current clinical treatment of RA, pharmaceuticals remain the primary option of treatment, primarily non-steroidal anti-inflammatory drugs, anti-rheumatic drugs, glucocorticoids and biological agents, amongst others; however, these drugs generally have other issues such as a high risk of relapse, complicated administration instructions resulting in poor adherence, development of drug resistance and expense. Botanicals and their extracts have been of great interest in the treatment of RA due to their high efficacy and lower risk of side effects. In the present study, HFLS cells were used as a blank control group and MH7A cells, which have a greater migratory and invasive capacity compared with HFLS cells (43), were used as a model group to investigate whether strychnine with *Atractylodes macrocephala* extract could affect the proliferation of MH7A cells and whether it was associated with the TLR4/NF-κB/NLRP3 pathway.

Materials and methods

Reagents. Strychnine and *Atractylodes macrocephalae* were purchased from Shandong Provincial Hospital of Traditional Chinese Medicine (Jinan, China). Strychnine (cat. no. DS0026; Chengdu Desite Biotechnology Co., Ltd.), Brucine (cat. no. DM0019; Chengdu Desite Biotechnology Co., Ltd.) Atractylenolide II (cat. no. DB0015; Chengdu Desite Biotechnology Co., Ltd.) and Methotrexate (cat. no. H31020644; Tonghua Maoxiang Pharmaceutical).

Cell culture. MH7A cells (cat. no. BNCC358158; BeNa Culture Collection; Beijing Beina Chunglian Institute of Biotechnology) were cultured in H-DMEM (cat. no. 12100046; Gibco; Thermo Fisher Scientific, Inc.) supplemented with 10% FBS (Gibco; Thermo Fisher Scientific, Inc.) and 1% penicillin mix (cat. no. P1400-100; Beijing Solarbio Science & Technology Co., Ltd.) at 37˚C in a humidified incubator supplied with 5% CO_2. HFLS cells (cat. no. JNO171-71; Jennio Biotech Co., Ltd.) were cultured in DMEM (cat. no. SH30243.01; Hyclone; Cytiva) supplemented with 10% FBS and 1% penicillin mix at 37˚C in a humidified incubator supplied with 5% CO_2. Both types of cells were purchased as the second-generation cell lines and passed through once in about 48 h, with subsequent experiments starting when both types of cells reached the 7th generation.

High-performance liquid chromatography (HPLC)-tandem mass spectrometry (MS/MS) analysis of chemical composition. The same batch of Strychnine and Atractylodes macrocephala was weighed, and 20 g Strychnine and 1,000 g Atractylodes macrocephala were weighed in 10 times the amount of water (w/v) (in the current study, 20 g of Strychnine and 200 g of water, 1,000 g of Atractylodes macrocephala and 10,000 g of water were used). The same method was adopted for a common decoction of 20 g Strychnine and 120 g *Atractylodes macrocephala*, and 20 g Strychnine and 240 g *Atractylodes macrocephala*. The drug was added to a round-bottom flask, about half of its capacity, and water was added to soak the surface of the restorative material by 1-2 cm, heated at 100˚C, refluxed and decocted and kept boiling for 1 h. After cooling to room temperature, a 0.22 microporous membrane was used for filtration. After decoction, 3 ml of the decoction was suspended in a 10-ml volumetric flask (3:7 ratio of decoction to HPLC grade methanol), diluted to the required scale using HPLC-grade methanol (cat. no. 34860;

Table I. Control component concentrations.

	Control mixture number					
Component	1	2	3	4	5	6
Strychnine, μg/ml	0.292	0.584	1.167	2.334	4.668	9.336
Brucine, μg/ml	0.272	0.545	1.089	2.178	4.356	8.712
Atractylodes II, μg/ml	0.260	0.519	1.038	2.076	4.152	8.304

Sigma-Aldrich; Merck KGaA) and transferred to a centrifuge tube at 25˚C, 1,610 x g for 15 min. When the centrifugation was completed, the supernatant was collected, the missing solution (the discarded precipitated fraction of liquid) was made up with methanol, the solution was filtered through a 0.22-μm microporous membrane and 2 μl of liquid was used for mass spectrometry analysis.

The strychnine, brucine, and Atractylenolide II were accurately weighed (all 1 mg) and dissolved in 1 ml HPLC grade methanol to obtain the 'master mix' of each substance. Subsequently, different proportions of the master mix were accurately aspirated and placed in the same 5-ml volumetric flask and mixed thoroughly to obtain the mixed reference substance solution for subsequent standard curve plotting. The concentrations of the resulting controls are presented in Table I.

The study was carried out on a TSQ Quantis triple-stage quadrupole mass (TSQ QUANTIS; Thermo Fisher Scientific, Inc.) with a Waters Symmetry-C18 (4.6x75 mm; 3.5 μm; Waters Corporation) column. The mobile phase was 1% formic acid (A)-acetonitrile (B) with gradient elution (0-35 min, 95-65% B; 35-40 min, 65% B; 40-55 min, 65-5% B; 55-56 min, 5-95% B; 56-60 min, 95% B) at a flow rate of 0.2 ml/min, column temperature of 30˚C and injection volume of 2.0 μl. The ion source was carried out using positive ion electrospray ionization (ESI) source with the sheath gas (N_2) flow rate set to 1.2 l/min; the auxiliary gas (N_2) was set to a flow rate of 0.09 l/min; the collision gas was argon (Ar) assigned to a flow rate of 2 m Torr; the atomization temperature was 300˚C; the atomizer pressure of 35 psi, the capillary temperature was 280˚C; and the spray voltage is 3,500 V. The scanning method was Selective Response Monitoring) for each ion. Strychnine m/z 395.16-243.97 with a collision energy of 37.73 eV, Brucine m/z 335.11-184 with a collision energy of 38.66 eV and Atractylenolide II m/z 232.3-158.1 with a collision energy of 17.93 eV. Data were acquired using Xcalibur software 4.1 (Thermo Fisher Scientific, Inc.), peak areas were calculated and standard curves were plotted using the concentration and peak area of the markers. AM group=the mixed standard. SS group=the liquid obtained by decoction of strychnine (20 g); S:A (1:6) group=liquid from decoction of strychnine (20 g) and *Atractylodes macrocephala* (120 g); S:A (1:12) liquid from decoction of strychnine (20 g) and *Atractylodes macrocephala* (240 g).

CCK-8 assay. Strychnine and Atractylenolide II were accurately weighed, and the two drugs were dissolved in the culture medium (H-DMEM medium containing 10% FBS and 1% penicillin-streptomycin) to the desired concentration. The Strychnine concentrations were 130, 390 and 780 μg/ml, while the concentrations of Atractylenolide II were 2, 20 and 40 μg/ml, followed by filtration through a 0.22-μm microporous filter membrane. Cells in the logarithmic phase of growth were digested for 1 min in a 5% CO_2 incubator at 37˚C with trypsin-EDTA digest (0.25%; cat. no. T1300-100; Beijing Solarbio Science & Technology Co., Ltd.) and made into cell suspensions. Subsequently, 100 μl of each of the aforementioned solutions were added to a 96-well plate and 100 μl of medium was used as a blank control. The plate was incubated overnight before dividing into seven groups: i) Control group; ii) strychnine 130 μg/ml group; iii) strychnine 390 μg/ml group; iv) strychnine 780 μg/ml group; v) Atractylenolide II 2 μg/ml; vi) Atractylenolide II 20 μg/ml; and vii) Atractylenolide II 40 μg/ml. After incubation for 0, 12, 24 or 48 h, a Cell Counting Kit-8 (CCK-8; cat. no. CP002; Signalway Antibody LLC) and serum-free H-DMEM were mixed in a 1:10 volume ratio, and 100 μl was added per well, after which cells were incubated for 1 h. Subsequently, the absorbance at 450 nm was measured using an enzyme marker (cat. no. DNM-9602; Beijing Prolong New Technology Co., Ltd.), and the values for each plate were recorded. A total of three replicates were used for each experimental group.

Flow cytometry analysis. Cells were divided into 7 groups: i) Control group (HLFS); ii) model group (MH7A); iii) methotrexate group (MTX, 0.1 mg/ml); iv) strychnine group (780 μg/ml); v) *Atractylodes macrocephala* group (12 μg/ml); vi) strychnine with *Atractylodes macrocephala* 1:6 group (S:A 1:6); and vii) strychnine with Atractylenolide II (S:A 1:6 component 780-12 μg/ml) group. After adding drugs, the above groups were put in a humidified incubator at 37˚C supplied with 5% CO_2 for 24 h. Among them, the strychnine and *Atractylodes macrocephala* group (S:A 1:6) consisted of two drugs, strychnine and *Atractylodes macrocephala*, two drugs co-decocted in a ratio of 1:6. The strychnine and atractylenolide II (S:A 1:6 component 780-12 μg/ml) group consisted of only two extracts, strychnine and Atractylenolide II, configured together. The media was removed from the drug-treated groups of cell cultures, the cells were washed with PBS, and the cells were digested using trypsin-EDTA digest. The cells were observed to be rounding under the microscope and the wall of the flask was gently tapped to observe when the cells fell off in a quicksand pattern. Medium was added to the flask to terminate the digestion. The cell cultures from the previous step were collected, mixed slightly and transferred to a centrifuge tube,

centrifuged at 1,000 x g, 25˚C for 5 min and then resuspend in PBS and drop resuspended onto the cell counting chamber for manual counting under a microscope. Between 50-100,000 resuspended cells were collected, centrifuged at 1,000 x g, 25˚C for 5 min, the supernatant was discarded and 200 μl Annexin V-FITC conjugate (cat. no. C1062S; Beyotime Institute of Biotechnology) was added and gently resuspended, mixed gently and incubated for 15 min at 4˚C in the dark. Subsequently, 5 μl propidium iodide staining solution was added, gently mixed and incubated for 5 min at 4˚C, while a tube without Annexin V-FITC and PI was used as the negative control. Flow cytometry analysis was performed using a BD Accuri C/6 flow cytometer (Becton, Dickinson and Company). Annexin V-FITC fluoresces green, corresponding to the FL1 detection channel; PI fluoresces red, corresponding to the FL2 detection channel. The analysis was performed using FlowJo 7.6.1 software (FlowJo LLC). A total of five replicates were used for each experimental group.

Immunofluorescence analysis. The dilution, batch number and supplier of the primary antibodies used were: TLR4 (1:800; cat. no. ab22048; Abcam), NF-κBP65, (1:1,200; cat. no. ab16502; Abcam) and NLRP3 (1:800; cat. no. ab214185; Abcam). The secondary antibodies used were IgG (Fluorescent dye FITC coupling; 1:100; cat. no. ZF-0316; OriGene Technologies, Inc.). The cells were digested with 0.25% trypsin-EDTA in a 5% CO_2 37˚C incubator for 1 min; the digested cell suspension was dropped onto a slide placed in the culture dish. After waiting for ~30 min for the cells to adhere to the wall, the medium (H-DMEM medium containing 10% FBS and 1% penicillin-streptomycin) was added and incubated in a 37˚C 5% CO_2 incubator for 2 h. The slide was removed after 2 h and rinsed three times with PBS for 2 min each time. Cells were fixed using 4% paraformaldehyde for 30 min at room temperature and washed, permeabilized using 0.5% Triton X-100 (in DPBS) for 20 min, followed by treatment with 3% methanolic hydrogen peroxide for 20 min at room temperature and then placed in PBS. A Pap Pen was used to draw circles surrounding the cells being examined on the slide to avoid the running and spreading of the fluid during staining. Goat serum sealant (no. ZLI-9022; ZSGB) was added dropwise for 20 min at room temperature to block the cells. The primary antibody was added dropwise and cells were incubated overnight at 4˚C, removed the next day and left for 20 min before adding the fluorescently labeled secondary antibody (IgG) dropwise. Cells were incubated in the dark for 20 min at 37˚C, placed in PBS, washed with water, air-dried and sealed with neutral resin. Overall, three replicates were used for each experimental group. Cells were observed using a fluorescence microscope at a magnification of 100x and 400x. Analysis of gray value with Image J 1.8.0 software (National Institutes of Health). An 'immunohistochemical score (IHS)' was calculated for each group by multiplying the percentage of stained cells with the score for staining intensity, using the following criteria: A=Grading the number of positive cells (0-1%=0; 1-10%=1; 10-50%=2; 50-80%=3; 80-100%=4); B=grading of the intensity of color development of positive cells [0 (negative), 1 (weakly positive), 2 (positive), 3 (strongly positive)]. Therefore, IHS=A x B.

Reverse transcription-quantitative PCR (RT-qPCR) assay. Total RNA was extracted from the tissue samples using an ultra-pure RNA extraction reagent (cat. no. 9108; Takara Bio, Inc.). Using the property that nucleic acids have strong absorption ~260 nm and proteins have strong absorption ~280 nm, the A260/A280 ratio of RNA was determined using a Nanodrop 2000 ultra-micro spectrophotometer; the ideal RNA purity A260/A280 should be in the range of 1.9-2.1. The residual genomic DNA in the RNA was digested using a gDNA Eraser (cat. no. RR047A; Takara Bio, Inc.). RT was performed using a Reverse Transcription kit according to the manufacturer's protocol (cat. no. DRRO47A; Takara Bio, Inc.). qPCR was performed using a SYBR Premix Ex Taq kit (cat. no. DRR420A; Takara Bio, Inc.) and amplification procedure: 95˚C for 30 sec, (95˚C for 5 sec; 60˚C for 34 sec) x40 cycles. The data were analyzed using the $2^{-\Delta\Delta Cq}$ method (44). Amplification was performed on an ABI 7500 fluorescent qPCR instrument. The sequences of the primers were: TLR4 forward, 5'-CAG GATGATGTCTGCCTCGC-3', and reverse, 5'-TGGTTTAGG GCCAAGTCTCC-3'; IκB kinase (IKKβ) forward, 5'-CTA AGGTGGAAGTGGCCCTC-3', and reverse, 5'-CTGGAT CCTACAAGGGACCG-3'; NF-κB p65 forward, 5'-TGAACC AGGGCATACCTGTG-3', and reverse 5'-CCCCTGTCACTA GGCGAGTT-3'; NLRP3 forward, 5'-GCTGGCATCTGG GGAAACCT-3', and reverse, 5'-GGTCCTTAGGCTTCG GTCCA-3'; TNF-α forward, 5'-GCTGCACTTTGGAGTGAT CG-3' and reverse, 5'-TCACTCGGGGTTCGAGAAGA-3'; and GAPDH forward, 5'-GCAAATTCCATGGCACCGTC-3' and reverse, 5'-AGCATCGCCCCACTTGATTT-3'. A total of five replicates were used for each experimental group.

Western blotting. The dilutions, batch numbers and suppliers of the antibodies used were: TLR4 (1:800; cat. no. ab22048; Abcam), p-NLRP3 (1:600; cat. no. AF4320; Affinity Biosciences), NLRP3 (1:800; cat. no. ab214185; Abcam), phosphorylated (p-)NF-κB P65 (1:600; cat. no. ab86299; Abcam), TNF-α (1:1,000; cat. no. ab6671; Abcam), IKKβ (1:800; cat. no. ab124957; Abcam), NF-κB P65 (1:1,200; cat. no. ab16502; Abcam) and β-actin (1:1,000; cat. no. TA-09; OriGene Technologies, Inc.). The cells were collected, centrifuged at 1,000 x g for 5 min at 25˚C to remove the original culture fluid, washed with PBS and lysed using 200 μl lysis solution (0.303 g Tris base, 0.4383 g NaCl, 0.05 g SDS, 40 ml H_2O; pH adjusted to 8.0 with HCl to a fixed volume of 50 ml) supplemented with PMSF. After centrifuging at 1,200 x g, 15˚C for 10 min to remove the cell debris, the protein concentration of each sample was determined using the Coomassie Blue Staining method (45), gently mixed with 5x protein gel loading buffer, denatured at 95˚C for 10 min and stored at -80˚C until required. The extracted total protein samples were removed from the -80˚C freezer and immediately inserted into ice and left to melt; according to the results of protein quantification, the corresponding volume of total protein was added to each lane (~30 μg protein/lane). Total protein was separated by SDS-PAGE on a 10% gel and transferred to a PVDF membrane. The PVDF membrane was carefully removed and placed in a sealing solution consisting of 100 ml 1X TBST (cat. no. T1085; Beijing Solarbio Science & Technology Co., Ltd.) and 5 g of skimmed milk powder (20:1) for 1 h at room temperature using a shaker with slow shaking, and then incubated with

the primary antibodies followed by the secondary antibody is horseradish peroxidase labelled goat anti-rabbit IgG (1:3,000; cat. no. ZB-2301; OriGene Technologies, Inc.), slow shaking at room temperature and away from light for 60 min. Analysis of gray values was performed using ImageJ 1.8.0 software (National Institutes of Health). The visualization reagents used are BeyoECL Plus luminescent liquids (cat. no. P0018S; Beyotime Institute of Biotechnology). A total of five replicates were used for each experimental group.

Statistical analysis. Data are expressed as mean ± standard deviation. All experiments were repeated at least three times. Differences between multiple groups were assessed using one-way analysis of variance and the Bonferroni post hoc test. When the data contains non-parametric data, the data are tested for normality. When the data conform to the normal distribution, the Kruskal-Wallis test was used for analysis. If the Kruskal-Wallis was significant, the Bonferroni method was used for analysis. All statistical analyses were performed in SPSS version 26.0 software (IBM Corp). $P<0.05$ was considered to indicate a statistically significant difference.

Results

The use of strychnine in combination with Atractylodes macrocephala can reduce the strychnine content. To determine the changes in the contents of strychnine, brucine and Atractylenolide II before and after the combination of Strychnos and *Atractylodes macrocephala*, the horizontal coordinate was set as the concentration of the control, the vertical coordinate was set as the peak area and the standard curves of the three chemical components were calculated and the linear regression was calculated. The regression equations and results of three chemical components were calculated respectively: y=2E+06x+88958, R2=0.9986; y=2E+06x-273931, R2=0.9996; y=115567x-4142.5, R2=0.9993. The value of R^2 was calculated to determine whether the standard curve has a good linear relationship. That is, the relationship between the concentration and the readout indicated a linear relationship, and when the $R^2>0.997$, the standard curve has a good linear relationship. From the aforementioned results, it was determined that the contents of strychnine, brucine and Atractylenolide II could be ascertained from the linear curve relationship established. A quantity of the control was injected six times in succession according to the aforementioned method and the concentrations of the three controls were subsequently measured. By calculating the relative standard deviation, the results exhibited <4% deviance, demonstrating that the method had good precision, reproducibility and accuracy. Precise quantities of each group of samples were injected three times and the external standard method was used to calculate the strychnine, brucine and Atractylenolide II levels. The results are presented in Table II. Compared with the SS group, the SA (1:6) and SA (1:12) groups contained lower levels of strychnine and brucine. The chromatograms of each group were obtained using HPLC-MS/MS (Fig. 1). Overall, the combination of strychnine and *Atractylodes macrocephala* could reduce the content of toxic components in strychnine and improve the safety of the medication.

Table II. Quantitative results of the effective components of brucine, strychnine and Atractylenolide.

Sample	Brucine, μg/ml	Strychnine, μg/ml	Atractylenolide II μg/ml
SS	129.212	127.234	Not detected
AM	0.222	0.0785	0.341
SA (1:6)	108.261	101.411	2.086
SA (1:12)	105.935	100.583	3.353

SS group, the liquid obtained by decoction of strychnine (20 g); AM group, the mixed standard; S:A (1:6) group, liquid from decoction of strychnine (20 g) and *Atractylodes macrocephalae* (120 g); S:A (1:12) liquid from decoction of strychnine (20 g) and *Atractylodes macrocephalae* (240 g).

MH7A cell proliferation is inhibited by strychnine. When MH7A cells were treated with 780 μg/ml strychnine for 24 h, there was a significant decrease in the proliferation of cells compared with the control group ($P<0.01$), and the effect was time-dependent with treatment for 48 h showing a further decrease. However, given the bigger decrease in the number of cells after 48, 24 h of treatment was used for all subsequent experiments. When MH7A cells were treated with 2, 20 and 40 μg/ml of Atractylenolide II for 12, 24 and 48 h, the cell proliferation demonstrated an upward trend compared with the control, which was significant for the 40 μg/ml of Atractylenolide II group at 48 h ($P<0.01$). This effect was also time-dependent, as no significant inhibitory trend was observed within 48 h of treatment, indicating that Atractylenolide II did not affect cell proliferation. Combined with the inhibitory effect of strychnine on cell proliferation, 24 h treatment was used for all subsequent experiments (Fig. 2). These results indicated that high doses of strychnine intervention MH7A cells at 48 h significantly impacted cell proliferation and, therefore, strychnine has some toxicity to cells.

Strychnine promotes apoptosis of synovial cells when combined with Atractylodes macrocephala. The cells started to adhere to the wall after 3-6 h of incubation; the morphology of the cells appeared fibrous before adherence to the wall. After 24 h of incubation, the distribution of cells indicated a certain direction and regularity. Both HFLS cells and MH7A cells possessed fibroblast-like characteristics, being spindle-shaped. There were no markedly different morphological changes in the cells under bright light microscopy after the addition of the drug treatment (Fig. 3).

The results of the flow cytometry assay revealed that the rate of early apoptosis was low in the Control and Model groups and did not differ significantly from each other. After treatment with MTX, strychnine, S-A1:6 and S-A1:6 component, the apoptosis rate of MH7A cells was significantly higher compared with that of the control group ($P<0.05$ or $P<0.01$; Fig. 4). These results indicated that the drugs in each group had no significant effect on the cell morphology but could significantly promote the apoptosis of MH7A cells after the intervention of two drugs.

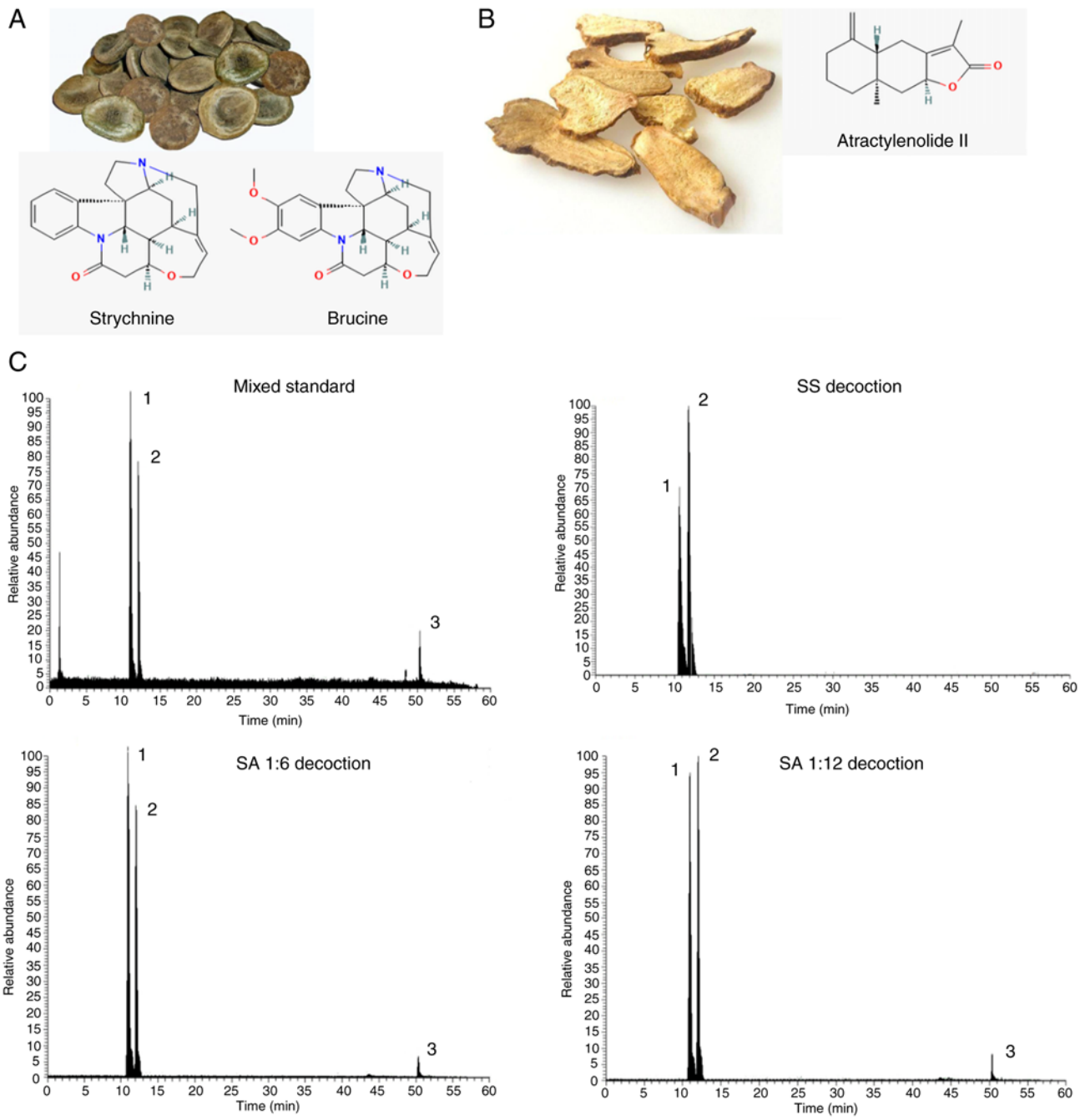

Figure 1. Image and chemical structure of strychnine and *Atractylodes macrocephala* alongside HPLC-MS/MS chromatography. (A) Strychnine chemical structure and formula of Strychnine and Brucine. (B) *Atractylodes macrocephala* chemical structure and formula of Atractylodes II. (C) HPLC-MS/MS chromatography (mixed standard, strychnine soup, strychnine and *Atractylodes macrocephala* 1:6 and strychnine and *Atractylodes macrocephala* 1:12). HPLC-MS/MS, high performance liquid chromatography with tandem mass spectrometry; AM group, the mixed standard. SS group, the liquid obtained by decoction of strychnine (20 g); SA (1:6) group, liquid from decoction of strychnine (20 g) and *Atractylodes macrocephala* (120 g); SA (1:12), liquid from decoction of strychnine (20 g) and Atractylodes macrocephala (240 g).

The strychnine and Atractylodes macrocephala combination inhibits the expression of TLR4, NF-κB and NLRP3. Compared with the control group, the expression levels of TLR4, NF-κB and NLRP3 were significantly enhanced in MH7A cells treated with IL-1β ($P<0.01$; Fig. 5). TLR4 expression was predominantly observed at the cell membrane, NLRP3 expression predominantly in the cytoplasm and NF-κB present at both. The number of positive cells was significantly reduced after MTX, S-A 1:6 and S-A 1:6 component treatment compared with the IL-1β-induced group ($P<0.05$ or $P<0.01$; Fig. 5). These results showed that the expression levels of TLR4, NF-κB and NLRP3 were significantly increased in MH7A cells induced by IL-1β, and the expression was significantly decreased after drug intervention. This demonstrated that the combination of the two drugs had the potential to inhibit the expression of TLR4, NF-κB and NLRP3.

The mRNA expression levels of TLR4, NF-κB and NLRP3 are significantly reduced after drug intervention. Compared with the control group, the mRNA expression of TLR4, IKKβ,

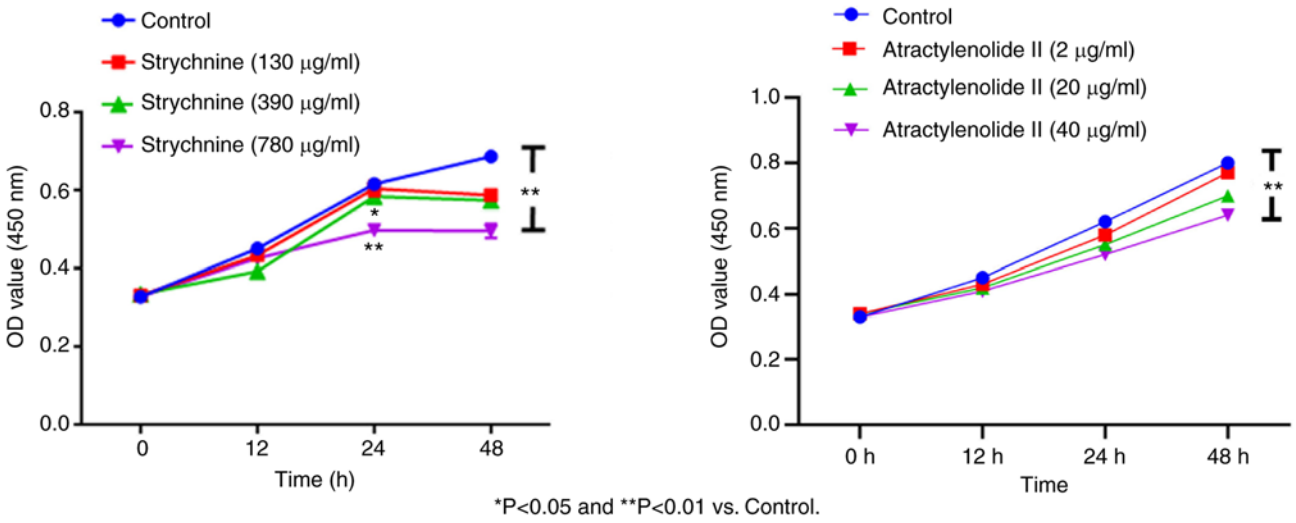

Figure 2. Cell Counting Kit-8 assay. Effect of different concentrations of strychnine and Atractylenolide II on the proliferation of MH7A cells at the same time. *P<0.05 and **P<0.01 vs. Control.

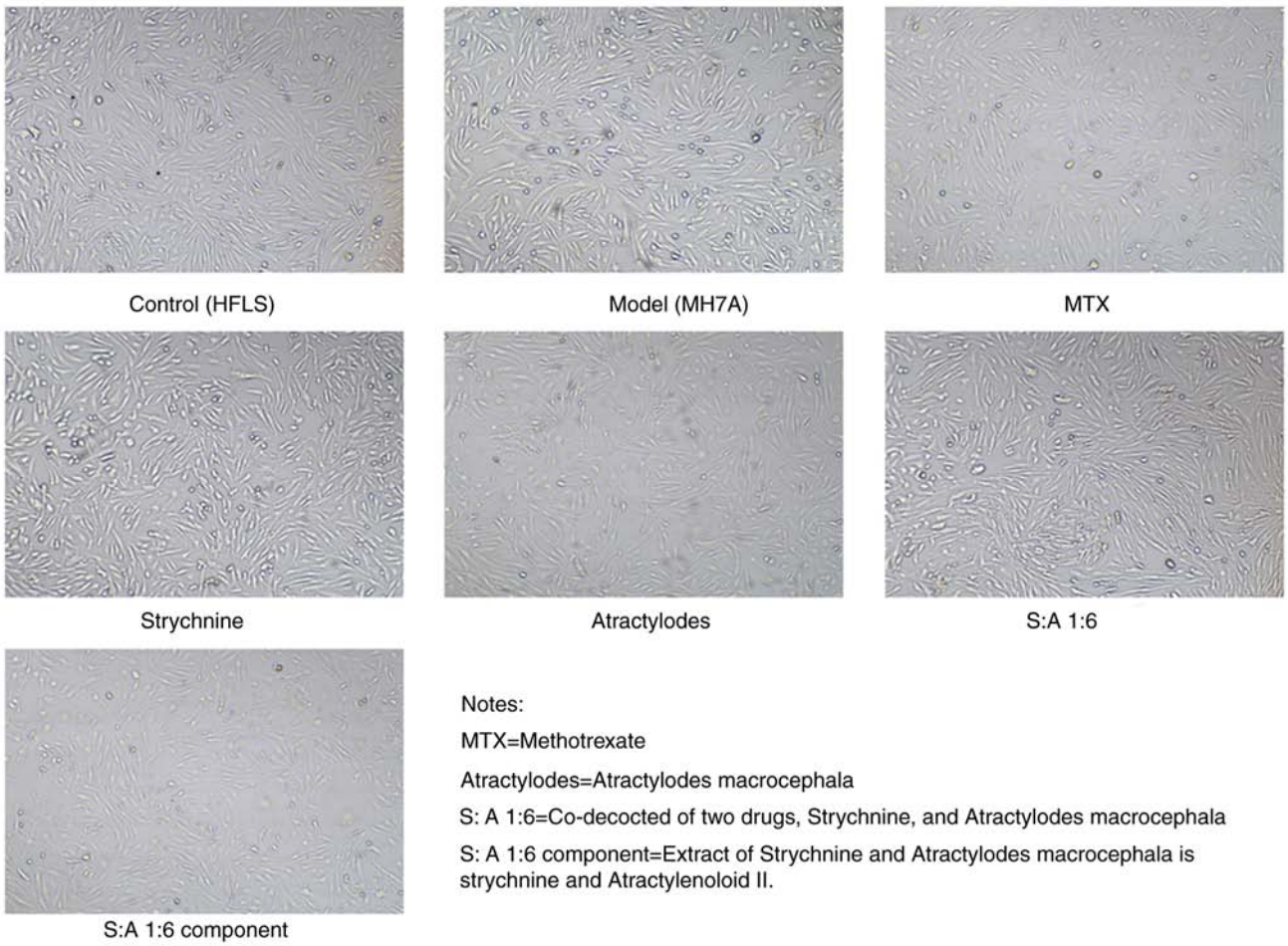

Figure 3. Images of the cell morphology after 24 h. MTX, Strychnine, *Atractylodes macrocephala*; S:A 1:6, co-decoction of two drugs, Strychnine and *Atractylodes macrocephala*; S:A 1:6 component group, extract of strychnine and Atractylenoloid II.

NF-κB, NLRP3 and TNF-α were significantly increased in IL-1β-induced MH7A cells (P<0.01; Fig. 6). Following MTX, S-A 1:6 and S-A 1:6 component treatment, expression levels of TLR4, IKKβ, NF-κB and NLRP3 were significantly reduced (P<0.01; Fig. 6). The results showed that the expression levels of TLR4, IKKβ, NF-κB, NLRP3 and TNF-α were significantly enhanced in IL-1β-mediated MH7A cells, and the expression levels were significantly decreased after the combination of the two drugs. This indicated that the combination of the two drugs has the potential to reduce the expression of these factors.

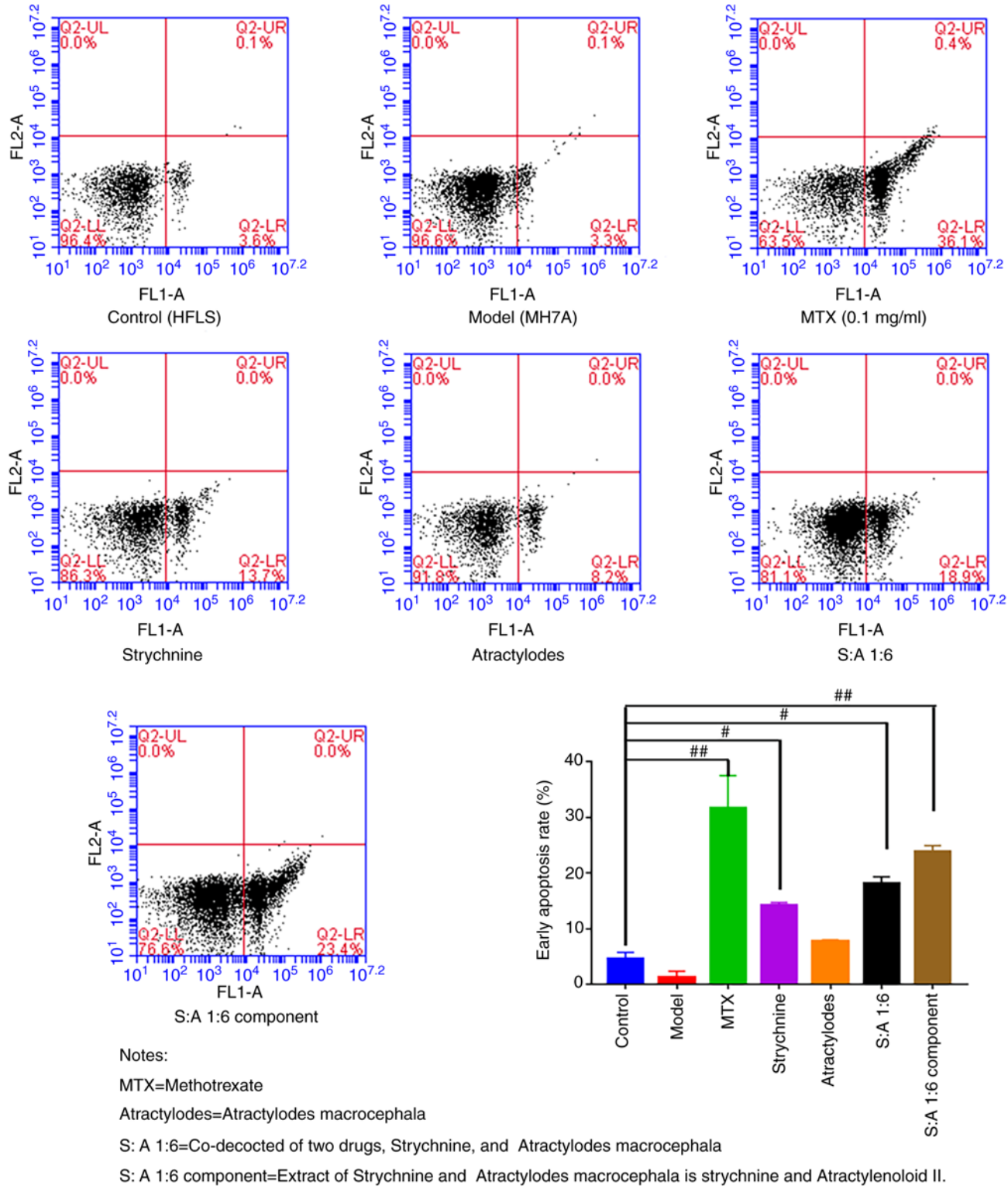

Figure 4. Apoptosis of MH7A cells following treatment with strychnine combined with *Atractylodes macrocephala*. n=5. $^{\#}$P<0.05 and $^{\#\#}$P<0.01 vs. Model. MTX, Strychnine, *Atractylodes macrocephala*; S:A 1:6, co-decoction of two drugs, Strychnine and *Atractylodes macrocephala*; S:A 1:6 component group, extract of strychnine and Atractylenoloid II.

Phosphorylation of TLR4 and NF-κB is significantly reduced following treatment with strychnine combined with white Atractylodes macrocephala. Compared with the control group, IL-1β-induced total protein expression levels of TLR4, IKKβ and NF-κB were significantly increased in MH7A cells (P<0.01; Fig. 7). The results showed that the ratios of pNF-κBP65/NF-κBP65 and pNLRP3/NLRP in MH7 A cells mediated by IL-1β were lower than those in the Control group. After drug intervention, the ratios of pNF-κBP65/NF-κBP65 and pNLRP3/NLRP increased. In addition, the phosphorylation levels of NF-κB and NLRP3 were elevated in the IL-1β-induced group compared with the Control group

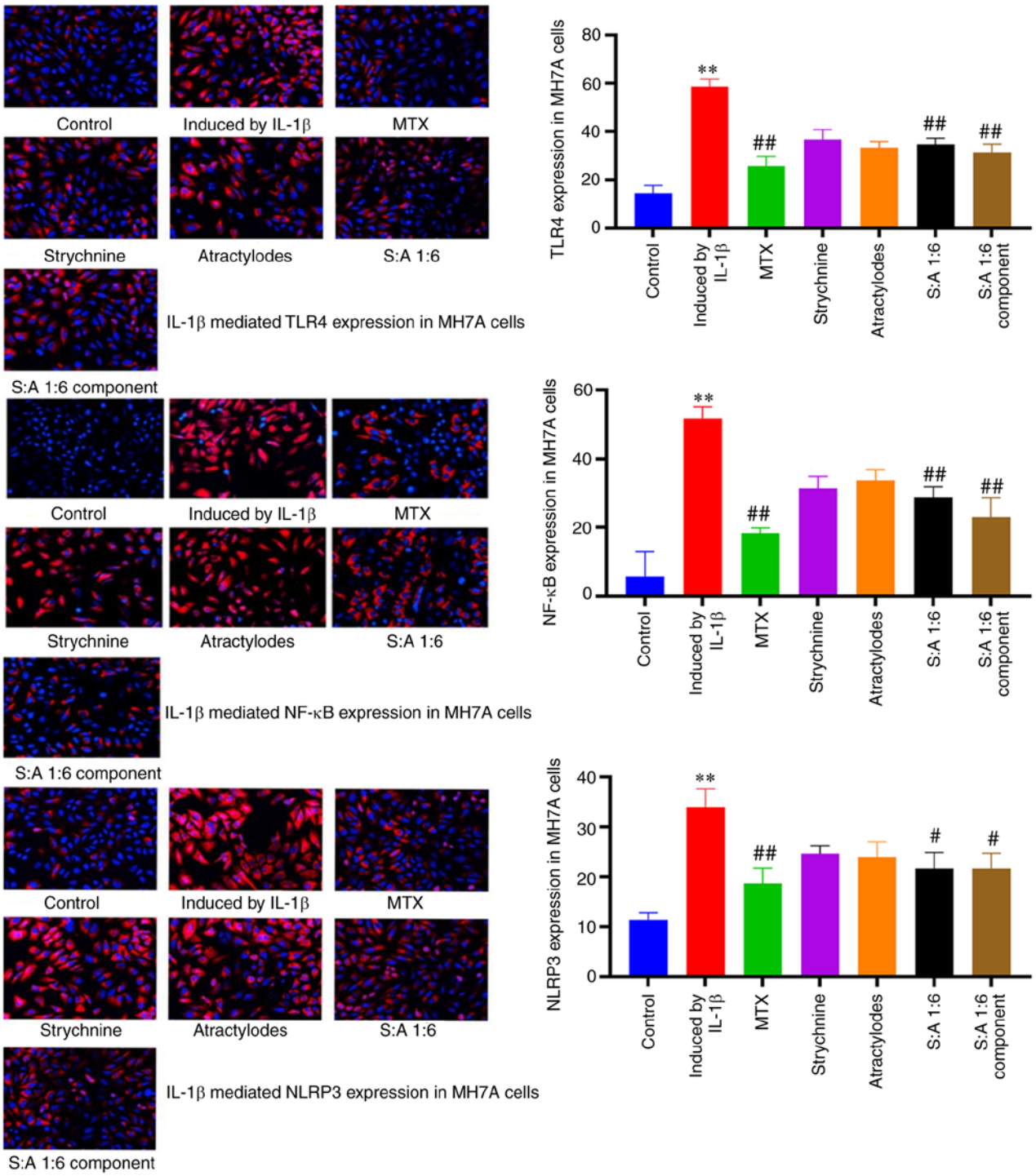

Figure 5. Immunofluorescence analysis of TLR4, NF-κB and NLRP3 expression and localization in MH7A cells following treatment with the strychnine and *Atractylodes macrocephala* combination. n=3. **P<0.01 vs. Control; $^{\#}$P<0.05 and $^{\#\#}$P<0.01 vs. induced by IL-1β. TLR4, Toll-like receptor 4; NF-κB; NLRP3, NLR family pyrin domain-containing 3 expression; MTX, Strychnine, *Atractylodes macrocephala*; S:A 1:6, co-decoction of two drugs, Strychnine and *Atractylodes macrocephala*; S:A 1:6 component group, extract of strychnine and Atractylenoloid II.

(P<0.01; Fig. 7). By contrast, expression levels of TLR4, p-NF-κB, NF-κB, p-NLRP3, TNF-α and IKKβ were significantly reduced after MTX, S-A 1:6 and S-A 1:6 component treatment (P<0.05 or P<0.01; Fig. 7). In addition, expression of NLRP3 was significantly reduced after MTX and N-A1:6 treatment (P<0.5; Fig. 7). The above results showed that the

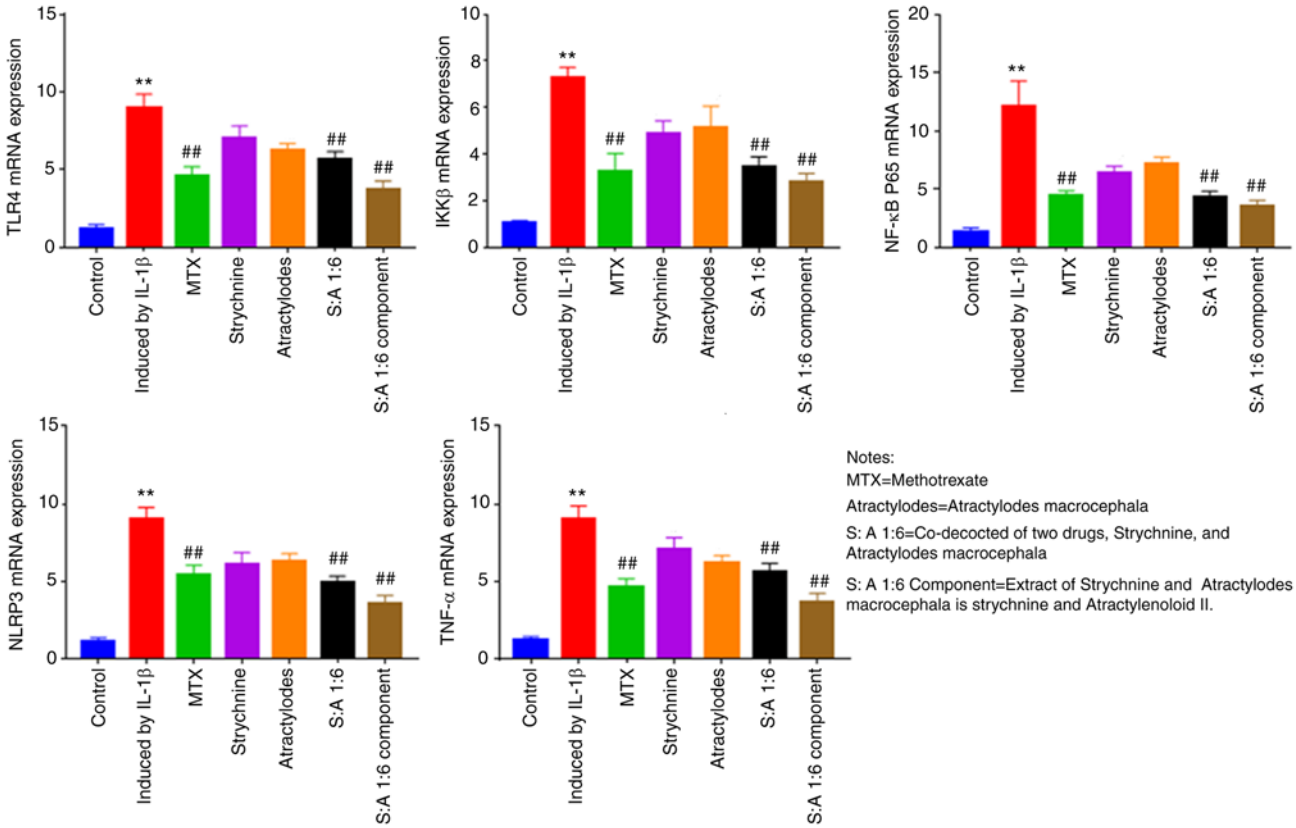

Figure 6. Effect of strychnine with *Atractylodes macrocephala* on IL-1β-mediated mRNA expression of TLR4, IKKβ, NF-κBp65, NLRP3 and TNF-α in MH7A cells. n=5. **P<0.01 vs. Control; $^{\#\#}$P<0.01 vs. Induced by IL-1β. TLR4, Toll-like receptor 4; IKK, IκB kinase; NF-κBp65; NLRP3, NLR family pyrin domain-containing 3; TNF-α expression; MTX, Strychnine, *Atractylodes macrocephala*; S:A 1:6, co-decoction of two drugs, Strychnine and *Atractylodes macrocephala*; S:A 1:6 component group, extract of strychnine and Atractylenoloid II.

combination of the two drugs could significantly inhibit the expression of TLR4, IKKβ and NF-κB in IL-1β cells.

Discussion

RA is a chronic, multifactorial inflammatory immune disease, the primary symptom of which is synovitis (46). In the early stages of the disease, pain and swelling of the joints are the primary manifestations, and, as the disease progresses, the joints become increasingly stiff and deformed. In severe cases this can lead to disability and thus seriously affect the quality of life of a patient; in addition, the cost of lengthy treatment adds to the burden of living. At present, the complexity of the pathogenesis of RA means that the current understanding of this disease and its underlying causes is incomplete, resulting in unsatisfactory treatment outcomes (47,48). Although non-steroidal anti-inflammatory drugs, glucocorticosteroids and biological agents (such as etanercept, infliximab and adalimumab.) have their own advantages in the treatment of RA, they also have a slow onset of action, are prone to relapse when stopped, are expensive, can induce gastrointestinal reactions and increase the risk of cardiovascular disease (49). It is therefore important to actively investigate alternative therapeutic approaches, such as complementary and alternative medicines, in addition to conventional medication.

Strychnine has been used in traditional Chinese medicines for >600 years and is widely used for rheumatism, swelling and pain (50,51). However, as toxic drugs, strychnine and brucine are both active ingredients and primary components that can cause poisoning and, in severe cases, it may lead to death (51). Therefore, in clinical practice, it is important to configure strychnine correctly to reduce its toxic component content. The combination of *Atractylodes macrocephala* and strychnine can reduce the level of toxic components of strychnine and enhance its analgesic and anti-inflammatory effects.

To the best of our knowledge, the present study was the first to reveal through CCK-8 experiments that when cells were treated with 780 μg/ml strychnine for 24 h, cell viability was significantly reduced compared with the control group, and this effect was time-dependent. Data from subsequent flow cytometry experiments demonstrated significant differences in the apoptotic rate of MH7A cells in the Control group following treatment with MTX, Strychnine, S:A 1:6 and S:A 1:6 component, indicating that the combination promoted apoptosis in synovial cells. In the follow-up experimental data, treatment with strychnine with *Atractylodes macrocephala* extract reduced the inflammatory response via IL-1β-induced activation of TLR4, NF-κB and NLRP3 inflammatory vesicles in MH7A cells.

TLR4/NF-κB/NLRP3 has been indicated to be involved in the inflammatory response and apoptosis (52,53). TLR-mediated signaling pathways are needed in the development of inflammation, and they play an integral role in the innate immune system as one of the most important pattern recognition systems (54), and modulation of TLR4 signaling

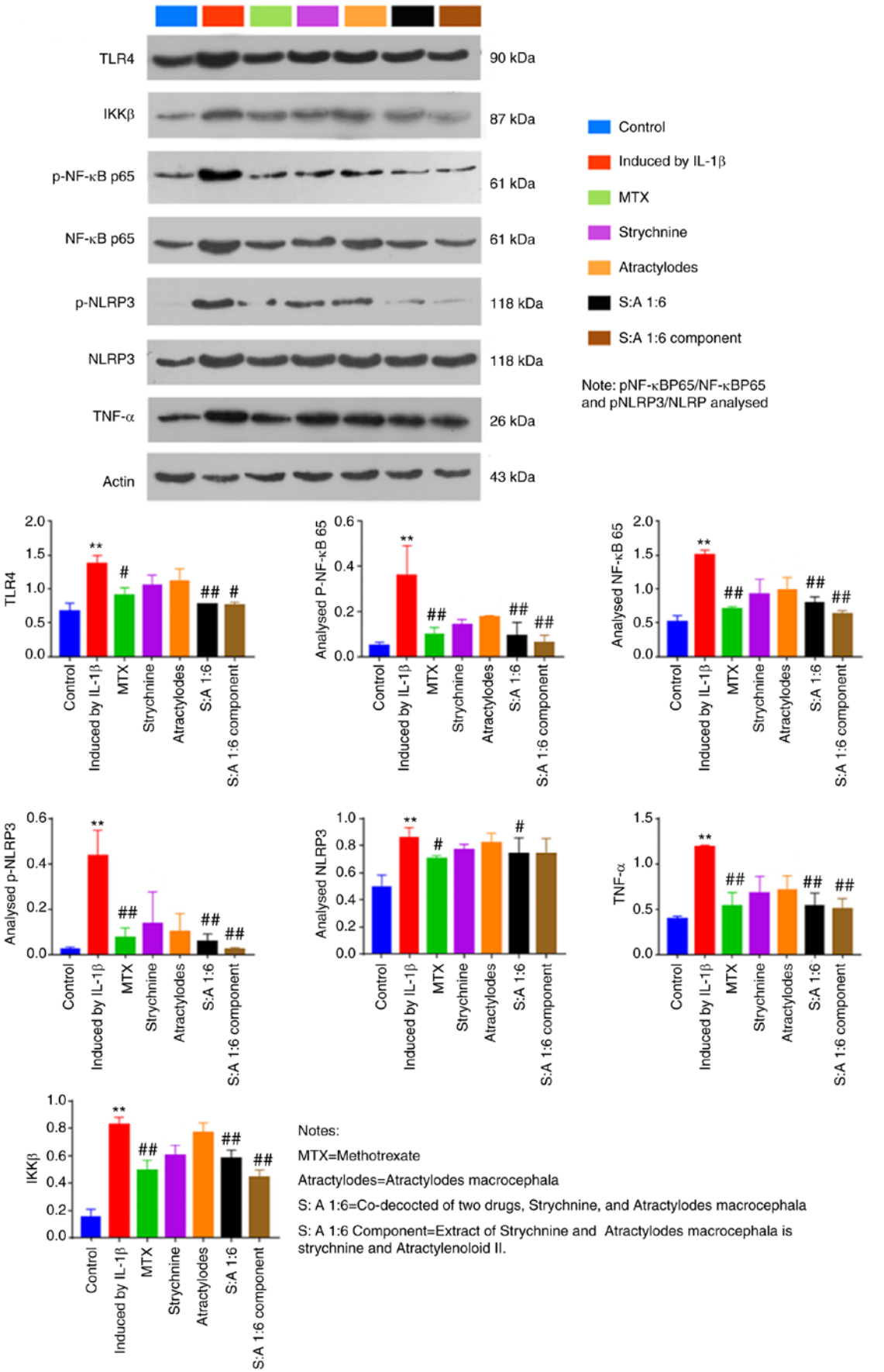

Figure 7. Effect of the strychnine and *Atractylodes macrocephala* combination on IL-1β-mediated expression of TLR4, NF-κB, IKKβ, NF-κB p65, p-NF-κB p65, NLRP3, p-NLRP3 and TNF-α in MH7A cells. n=5. **P<0.01 vs. Control; $^{\#}$P<0.05 and $^{\#\#}$P<0.01 vs. Induced by IL-1β. TLR4, Toll-like receptor 4; IKK, IκB kinase; p-NF-κB p65; NF-κB p65. NLRP3, NLR family pyrin domain-containing 3; p-, phosphorylated; TNF-α expression;, MTX, methotrexate; Strychnine; *Atractylodes macrocephala*; S: A 1:6 co-decocted of two drugs co-decocted of two drugs, Strychnine, and *Atractylodes macrocephala*, S: A 1:6 extract of Strychnine and *Atractylodes macrocephala* is strychnine and Atractylenoloid II component group.

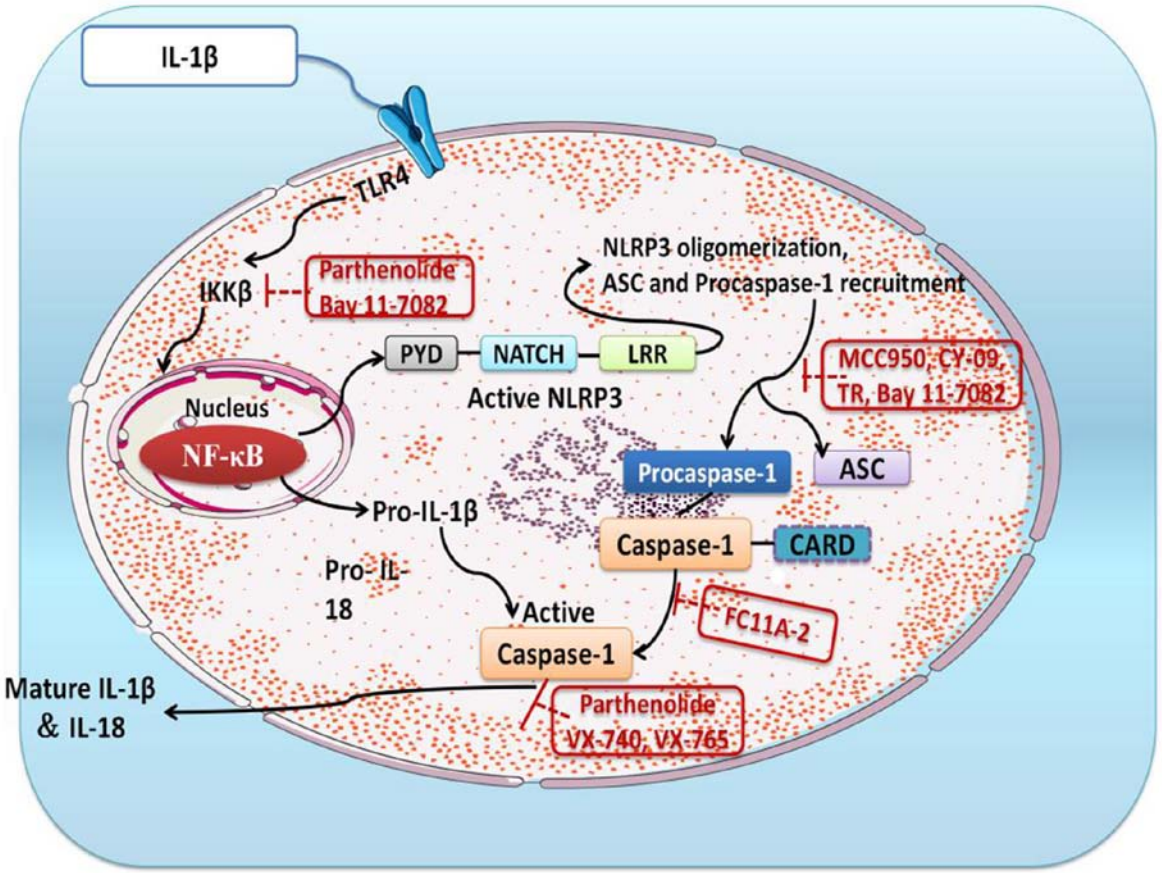

Figure 8. Diagram of the TLR4/NF-κB/NLRP3 signaling pathway. IKK, IκB kinase; NLRP3, NLR family pyrin domain-containing 3; TLR4, Toll-like receptor 4; PYD, pyrin domain; LRR, leucine-rich repeat domain; ASC, apoptosis-associated speck-like protein; CARD, caspase recruitment domain; FC11A-2, 1-ethyl-5-methyl-2-phenyl-1H-benzo[d]imidazole.

pathways may have potential therapeutic advantages in the treatment of RA.

The present study demonstrated that in IL-1β-mediated MH7A cells, the TLR4 receptor was primarily expressed at the cell membrane surface. It has been established that when TLR4 is activated it induces inflammatory cells to secrete large quantities of inflammatory cytokines such as TNF-α, IL-1β and IL-18 (55,56). IL-1β orchestrates the immune response at the local and systemic level, stimulating cells to secrete other inflammatory cytokines (57). From the aforementioned experiments, it was hypothesized that strychnine combined with *Atractylodes macrocephala* extract is a potent anti-inflammatory agent and its inhibitory effect on inflammation may be associated with the TLR4 signaling pathway.

When IL-1β binds to the TLR4 receptor, the NF-κB pathway is activated, and this is associated with pro-inflammatory cytokine production (58). Therefore, NF-κB is considered a key target in the treatment of inflammatory diseases (59). IKK is a common transcription factor-activating protein, composed of IKKα, IKKβ and the IKK-related kinases TBK1 and IKKε (60). These kinases are considered to be major regulators of inflammation and innate immunity through the control of transcription factors such as NF-κB (61,62). When the TLR4 signaling pathway is activated by IL-1β and inflammatory factors are released to act on IKK, the heterodimeric protein NF-κB is released following phosphorylation of the IκBα protein bound to NF-κB in the cytoplasmic matrix. This allows it to be specifically recognized by E3 ubiquitin ligase, which then tags it with the degradation signal K48-type polyubiquitin chains, which are subsequently specifically recognized and degraded by the 26S proteasome (63). In the present study, strychnine combined with *Atractylodes macrocephala* extract significantly inhibited IL-1β-induced activation of NF-κB and NLRP3 phosphorylation in MH7A cells, suggesting that Strychnine combined with *Atractylodes macrocephala* extract may reduce the levels of pro-inflammatory cytokines through the TLR4/NF-κB/NLRP3 pathway.

The NLR family of proteins are inflammatory vesicles present in germline-encoded pattern recognition receptors (64) and include NLRP1, NLRP3 and NLRP4 (65,66). Of these, NLRP3 has been extensively studied on the previous and consists of three components, NLRP3, ASC and caspase-1 (67-69). There is evidence that NLRP3 regulates the production of pro-inflammatory cytokines (70). The activation of caspase-1 is conditioned by the conversion of pro-IL-1β to mature IL-1β, which is dependent on NLPR3 inflammatory vesicles (71). When it is activated, the NLPR3 protein will induce translocation and activate pro-caspase-1 upon binding to the ASC adapter (72). The present study revealed that strychnine with *Atractylodes macrocephala* extract could effectively inhibit TLR4, pNF-κBp65, NF-κBp65, pNLRP3, TNF-κ and IKKβ protein expression levels in MH7A cells and, thus, it was hypothesized that this may be due to downregulation of NLPR3 protein expression and inhibition of ASC adapter and caspase-1

activity. Strychnine combined with *Atractylodes macrocephala* extract was able to reduce IL-1β-stimulated production of other inflammatory factors (such as IL-1β and IL-18) in MH7A cells, and the combination of the two inhibited NLRP3 inflammatory vesicles. A simplified overview of the above signaling pathway is presented in Fig. 8.

In conclusion, the enhanced inhibitory effect of *Atractylodes macrocephala* extract with strychnine on the inflammatory response of MH7A cells was identified in the present study. The results revealed that *Atractylodes macrocephala* extract with strychnine promoted apoptosis of synovial cells and inhibited the expression of TLR4, the NF-κB signaling pathway, NLRP3 and activation of caspase-1 under IL-1β induction. These results suggested that strychnine combined with *Atractylodes macrocephala* extract exerted its anti-inflammatory effects by inhibiting the NF-κB signaling pathway and NLRP3 inflammatory vesicles. This suggested that strychnine in combination with *Atractylodes macrocephala* extract may have potential in the treatment of RA as well as other inflammation-related diseases.

Future experiments are planned to establish an animal model of rheumatoid arthritis by adjuvant in Wistar rats to obtain an inflammatory model group. The administration groups will grouped in the same way as in the cellular experiments, and the efficacy of the combination of the two will first be verified using pharmacodynamic experiments, such as foot and plantar swelling scoring and hot plate in rats. The changes of inflammatory index factors in rat serum will then analyzed by ELISA assay to verify whether strychnine and *Atractylodes macrocephala* had anti-inflammatory effects. Finally, the relevant indexes will be detected using immunohistochemistry using the NF-κB inhibitor Bay 11-7082 (73-75). RT-qPCR assay and western blotting will be performed to verify whether the combination of strychnine and *Atractylodes macrocephala* has anti-inflammatory effects through TLR4/NF-κB/NLRP3 signaling pathway in treating RA, and to seek evidence that Strychnos and *Atractylodes macrocephala* II are the main active ingredients in the treatment.

Acknowledgements

Not applicable.

Funding

No funding was received.

Availability of data materials

The datasets used and/or analyzed during the current study are available from the corresponding author on reasonable request.

Authors' contributions

YG, XDL and YT conceived and designed the study. YG and DX performed the experiments and analyzed the results. YG, DX and XDL were involved in editing the graphs and drafting the manuscript. YT and XDL confirm the authenticity of all the raw data. All authors read and approved the final manuscript.

Ethics approval and consent to participate

Not applicable.

Patient consent to participate

Not applicable.

Competing interests

The authors declare that they have no competing interests.

References

1. Liu W, Zhang Y, Zhu W, Ma C, Ruan J, Long H and Wang Y: Sinomenine inhibits the progression of rheumatoid arthritis by regulating the secretion of inflammatory cytokines and monocyte/macrophage subsets. Front Immunol 9: 2228, 2018.
2. Korczowska I: Rheumatoid arthritis susceptibility genes: An overview. World J Orthop 5: 544-549, 2014.
3. Khurana R and Berney SM: Clinical aspects of rheumatoid arthritis. Pathophysiology 12: 153-165, 2005.
4. Scott DL, Wolfe F and Huizinga TW: Rheumatoid arthritis. Lancet 376: 1094-1108, 2010.
5. Kotake S, Sato K, Kim KJ, Takahashi N, Udagawa N, Nakamura I, Yamaguchi A, Kishimoto T, Suda T and Kashiwazaki S: Interleukin-6 and soluble interleukin-6 receptors in the synovial fluids from rheumatoid arthritis patients are responsible for osteoclast-like cell formation. J Bone Miner Res 11: 88-95, 1996.
6. Koopman FA, Chavan SS, Miljko S, Grazio S, Sokolovic S, Schuurman PR, Mehta AD, Levine YA, Faltys M, Zitnik R, *et al*: Vagus nerve stimulation inhibits cytokine production and attenuates disease severity in rheumatoid arthritis. Proc Natl Acad Sci USA 113: 8284-8289, 2016.
7. Thomas R and Cope AP: Oxford textbook of rheumatology. Oxford University Press, Oxford, UK, 2015.
8. McInnes IB and Schett G: The pathogenesis of rheumatoid arthritis. N Engl J Med 365: 2205-2219, 2011.
9. Syngle D, Singh A and Verma A: Impact of rheumatoid arthritis on work capacity impairment and its predictors. Clin Rheumatol 39: 1101-1109, 2020.
10. van den Bemt BJ, Zwikker HE and van den Ende CH: Medication adherence in patients with rheumatoid arthritis: A critical appraisal of the existing literature. Expert Rev Clin Immunol 8: 337-351, 2012.
11. Korani S, Korani M, Butler AE and Sahebkar A: Genetics and rheumatoid arthritis susceptibility in Iran. J Cell Physiol 234: 5578-5587, 2019.
12. Lee SY, Cho ML, Oh HJ, Ryu JG, Park MJ, Jhun JY, Park MK, Stone JC, Ju JH, Hwang SY, *et al*: Interleukin-2/anti-interleukin-2 monoclonal antibody immune complex suppresses collagen-induced arthritis in mice by fortifying interleukin-2/STAT5 signaling pathways. Immunology 137: 305-316, 2012.
13. Cooles FA, Isaacs JD and Anderson AE: Treg cells in rheumatoid arthritis: An update. Curr Rheumatol Rep 15: 352, 2013.
14. Pan F, Zhu L, Lv H and Pei C: Quercetin promotes the apoptosis of fibroblast-like synoviocytes in rheumatoid arthritis by upregulating lncRNA MALAT1. Int J Mol Med 38: 1507-1514, 2016.
15. Yang J, Zhao F and Nie J: Anti-rheumatic effects of Aconitum leucostomum Worosch. On human fibroblast-like synoviocyte rheumatoid arthritis cells. Exp Ther Med 14: 453-460, 2017.
16. McInnes IB and Schett G: Pathogenetic insights from the treatment of rheumatoid arthritis. Lancet 389: 2328-2337, 2017.
17. Zhu YG and Qu JM: Toll like receptors and inflammatory factors in sepsis and differential expression related to age. Chin Med J (Engl) 120: 56-61, 2007.
18. Qing YF, Zhang QB, Zhou JG and Jiang L: Changes in toll-like receptor (TLR)4-NFκB-IL1β signaling in male gout patients might be involved in the pathogenesis of primary gouty arthritis. Rheumatol Int 34: 213-220, 2014.

19. Chang YY, Jean WH, Lu CW, Shieh JS, Chen ML and Lin TY: Nicardipine inhibits priming of the NLRP3 inflammasome via suppressing LPS-induced TLR4 expression. Inflammation 43: 1375-1386, 2020.
20. Martinon F, Burns K and Tschopp J: The inflammasome: A molecular platform triggering activation of inflammatory caspases and processing of proIL-beta. Mol Cell 10: 417-426, 2002.
21. Agostini L, Martinon F, Burns K, McDermott MF, Hawkins PN and Tschopp J: NALP3 forms an IL-1beta-processing inflammasome with increased activity in Muckle-Wells autoinflammatory disorder. Immunity 20: 319-325, 2004.
22. Schroder K and Tschopp J: The inflammasomes. Cell 140: 821-832, 2010.
23. Strowig T, Henao-Mejia J, Elinav E and Flavell R: Inflammasomes in health and disease. Nature 481: 278-286, 2012.
24. Xu XY, Cai BC, Pan Y and Wang TS: Pharmacokinetics of the alkaloids from the processed seeds of *Strychnos nux-vomica* in rats. Yao Xue Xue Bao 38: 458-461, 2003 (In Chinese).
25. Tang M, Zhu WJ, Yang ZC and He CS: Brucine inhibits TNF-α-induced HFLS-RA cell proliferation by activating the JNK signaling pathway. Exp Ther Med 18: 735-740, 2019.
26. Shu G, Mi X, Cai J, Zhang X, Yin W, Yang X, Li Y, Chen L and Deng X: Brucine, an alkaloid from seeds of *Strychnos nux-vomica* Linn., represses hepatocellular carcinoma cell migration and metastasis: The role of hypoxia inducible factor 1 pathway. Toxicol Lett 222: 91-101, 2013.
27. Rao PS and Prasad MN: *Strychnos nux-vomica* root extract induces apoptosis in the human multiple myeloma cell line-U266B1. Cell Biochem Biophys 66: 443-450, 2013.
28. Chen J, Qu Y, Wang D, Peng P, Cai H, Gao Y, Chen Z and Cai B: Pharmacological evaluation of total alkaloids from nux vomica: Effect of reducing strychnine contents. Molecules 19: 4395-4408, 2014.
29. Li Y, Liu Y, Shao Y, Zhang F, Liu W, Liang X and Chen L: Mechanism of action of strychni semen for treating rheumatoid arthritis and methods for attenuating the toxicity. Comb Chem High Throughput Screen 25: 587-606, 2022.
30. Guo R, Wang T, Zhou G, Xu M, Yu X, Zhang X, Sui F, Li C, Tang L and Wang Z: Botany, phytochemistry, pharmacology and toxicity of *Strychnos nux-vomica* L.: A review. Am J Chin Med 46: 1-23, 2018.
31. Qin JM, Yin PH, Li Q, Sa ZQ, Sheng X, Yang L, Huang T, Zhang M, Gao KP, Chen QH, *et al*: Anti-tumor effects of brucine immuno-nanoparticles on hepatocellular carcinoma. Int J Nanomedicine 7: 369-379, 2012.
32. Chen J, Hou T, Fang Y, Chen ZP, Liu X, Cai H, Lu TL, Yan GJ and Cai BC: HPLC determination of strychnine and brucine in rat tissues and the distribution study of processed semen strychni. Yakugaku Zasshi 131: 721-729, 2011.
33. Dai J, Liu J, Zhang M, Yu Y and Wang J: Network toxicology and molecular docking analyses on strychnine indicate CHRM1 is a potential neurotoxic target. BMC Complement Med Ther 22: 273, 2022.
34. Otter J and D'Orazio JL: Strychnine toxicity. In: StatPearls [Internet]. Treasure Island (FL): StatPearls Publishing, 2022.
35. Lu L, Huang R, Wu Y, Jin JM, Chen HZ, Zhang LJ and Luan X: Brucine: A review of phytochemistry, pharmacology, and toxicology. Front Pharmacol 11: 377, 2020.
36. Zhao C, Li E, Wang Z, Tian J, Dai Y, Ni Y, Li F, Ma Z and Lin R: Nux vomica exposure triggered liver injury and metabolic disturbance in zebrafish larvae. Zebrafish 15: 610-628, 2018.
37. Fan Y, Liu S, Chen X, Feng M, Song F and Gao X: Toxicological effects of nux vomica in rats urine and serum by means of clinical chemistry, histopathology and ^{1}H NMR-based metabonomics approach. J Ethnopharmacol 210: 242-253, 2018.
38. Li Y, Wang J, Xiao Y, Wang Y, Chen S, Yang Y, Lu A and Zhang S: A systems pharmacology approach to investigate the mechanisms of action of semen strychni and Tripterygium wilfordii Hook F for treatment of rheumatoid arthritis. J Ethnopharmacol 175: 301-314, 2015.
39. Lü D, Jiang Q, Zhang J, Zeng R, Liao Z and Liang X: Effect of baizhu (rhizoma atractylodis macrocephalae) extract on intestinal absorption of brucine and strychnine in vitro and in situ. J Tradit Chin Med 40: 562-570, 2020.
40. Emery P, Breedveld FC, Hall S, Durez P, Chang DJ, Robertson D, Singh A, Pedersen RD, Koenig AS and Freundlich B: Comparison of methotrexate monotherapy with a combination of methotrexate and etanercept in active, early, moderate to severe rheumatoid arthritis (COMET): A randomised, double-blind, parallel treatment trial. Lancet 372: 375-382, 2008.
41. Friedman B and Cronstein B: Methotrexate mechanism in treatment of rheumatoid arthritis. Joint Bone Spine 86: 301-307, 2019.
42. Alarcón GS, Tracy IC and Blackburn WJ Jr: Methotrexate in rheumatoid arthritis. Toxic effects as the major factor in limiting long-term treatment. Arthritis Rheum 32: 671-676, 1989.
43. Yu Z, Liu H, Fan J, Chen F and Liu W: MicroRNA-155 participates in the expression of LSD1 and proinflammatory cytokines in rheumatoid synovial cells. Mediators Inflame 2020: 4092762, 2020.
44. Livak KJ and Schmittgen TD: Analysis of relative gene expression data using real-time quantitative PCR and the 2(-Delta Delta C(T)) method. Methods 25: 402-408, 2001.
45. Brunelle JL and Green R: Coomassie blue staining. Methods Enzymol 541: 161-167, 2014.
46. Dörner T, Vital EM, Ohrndorf S, Alten R, Bello N, Haladyj E and Burmester G: A narrative literature review comparing the key features of musculoskeletal involvement in rheumatoid arthritis and systemic lupus erythematosus. Rheumatol Ther 9: 781-802, 2022.
47. Radu AF and Bungau SG: Management of rheumatoid arthritis: An overview. Cells 10: 2857, 2021.
48. Chauhan K, Jandu JS, Goyal A and Al-Dhahir MA: Rheumatoid arthritis. In: StatPearls. StatPearls Publishing, Treasure Island, FL, 2022.
49. Zhong Y, Lai D, Zhang L, Lu W, Shang Y and Zhou H: The effects of moxibustion on PD-1/PD-L1-related molecular expression and inflammatory cytokine levels in RA rats. Evid Based Complement Alternat Med 2021: 6658946, 2021.
50. Li S, Chu Y, Zhang R, Sun L and Chen X: Prophylactic neuroprotection of total glucosides of paeoniae radix alba against semen strychni-induced neurotoxicity in rats: Suppressing oxidative stress and reducing the absorption of toxic components. Nutrients 10: 514, 2018.
51. Tong HF, Chan CY, Ng SW and Mak TWL: Strychnine poisoning due to traditional Chinese medicine: A case series. F1000Res 10: 924, 2021.
52. Cao B, Wang T, Qu Q, Kang T and Yang Q: Long noncoding RNA SNHG1 promotes neuroinflammation in Parkinson's disease via regulating miR-7/NLRP3 pathway. Neuroscience 388: 118-127, 2018.
53. Bachmaier K, Toya S, Gao X, Triantafillou T, Garrean S, Park GY, Frey RS, Vogel S, Minshall R, Christman JW, *et al*: E3 ubiquitin ligase Cblb regulates the acute inflammatory response underlying lung injury. Nat Med 13: 920-926, 2007.
54. Xiang P, Chen T, Mou Y, Wu H, Xie P, Lu G, Gong X, Hu Q, Zhang Y and Ji H: NZ suppresses TLR4/NF-κB signalings and NLRP3 inflammasome activation in LPS-induced RAW264.7 macrophages. Inflamm Res 64: 799-808, 2015.
55. Pålsson-McDermott EM and O'Neill LAJ: Signal transduction by the lipopolysaccharide receptor, Toll-like receptor-4. Immunology 113: 153-162, 2004.
56. Wang Y, Cui Y, Cao F, Qin Y, Li W and Zhang J: Ganglioside GD1a suppresses LPS-induced pro-inflammatory cytokines in RAW264.7 macrophages by reducing MAPKs and NF-κB signaling pathways through TLR4. Int Immunopharmacol 28: 136-145, 2015.
57. Malik A and Kanneganti TD: Function and regulation of IL-1α in inflammatory diseases and cancer. Immunol Rev 281: 124-137, 2018.
58. Zusso M, Lunardi V, Franceschini D, Pagetta A, Lo R, Stifani S, Frigo AC, Giusti P and Moro S: Ciprofloxacin and levofloxacin attenuate microglia inflammatory response via TLR4/NF-kB pathway. J Neuroinflammation 16: 148, 2019.
59. Wu XL, Liou CJ, Li ZY, Lai XY, Fang LW and Huang WC: Sesamol suppresses the inflammatory response by inhibiting NF-κB/MAPK activation and upregulating AMP kinase signaling in RAW 264.7 macrophages. Inflamm Res 64: 577-588, 2015.
60. Antonia RJ, Hagan RS and Baldwin AS: Expanding the view of IKK: New substrates and new biology. Trends Cell Biol 31: 166-178, 2021.
61. Wu J and Chen ZJ: Innate immune sensing and signaling of cytosolic nucleic acids. Annu Rev Immunol 32: 461-488, 2014.
62. Helgason E, Phung QT and Dueber EC: Recent insights into the complexity of Tank-binding kinase 1 signaling networks: the emerging role of cellular localization in the activation and substrate specificity of TBK1. FEBS Lett 587: 1230-1237, 2013.
63. Di Rita A, Peschiaroli A, D Acunzo P, Strobbe D, Hu Z, Gruber J, Nygaard M, Lambrughi M, Melino G, Papaleo E, *et al*: HUWE1 E3 ligase promotes PINK1/PARKIN-independent mitophagy by regulating AMBRA1 activation via IKKα. Nat Commun 9: 3755, 2018.

64. Takeuchi O and Akira S: Pattern recognition receptors and inflammation. Cell 140: 805-820, 2010.
65. Lamkanfi M and Dixit VM: Mechanisms and functions of inflammasomes. Cell 157: 1013-1022, 2014.
66. Sharma D and Kanneganti TD: The cell biology of inflammasomes: Mechanisms of inflammasome activation and regulation. J Cell Biol 213: 617-629, 2016.
67. Li Z, Guo J and Bi L: Role of the NLRP3 inflammasome in autoimmune diseases. Biomed Pharmacother 130: 110542, 2020.
68. Mangan MSJ, Olhava EJ, Roush WR, Seidel HM, Glick GD and Latz E: Targeting the NLRP3 inflammasome in inflammatory diseases. Nat Rev Drug Discov 17: 588-606, 2018.
69. Shao BZ, Xu ZQ, Han BZ, Su DF and Liu C: NLRP3 inflammasome and its inhibitors: A review. Front Pharmacol 6: 262, 2015.
70. Luo YP, Jiang L, Kang K, Fei DS, Meng XL, Nan CC, Pan SH, Zhao MR and Zhao MY: Hemin inhibits NLRP3 inflammasome activation in sepsis-induced acute lung injury, involving heme oxygenase-1. Int Immunopharmacol 20: 24-32, 2014.
71. Sun L, Ma W, Gao W, Xing Y, Chen L, Xia Z, Zhang Z and Dai Z: Propofol directly induces caspase-1-dependent macrophage pyroptosis through the NLRP3-ASC inflammasome. Cell Death Dis 10: 542, 2019.
72. Chao LK, Lin CH, Chiu HW, Wong WT, Chiu HW, Tasi YL, Kuo YH, Chiu YC, Liu ML, Ho CL and Hua KF: Peroxyauraptenol inhibits inflammation and NLRP3 inflammasome activation by inhibiting reactive oxygen species generation and preserving mitochondrial integrity. J Agric Food Chem 63: 1210-1219, 2015.
73. Lee J, Rhee MH, Kim E and Cho JY: BAY 11-7082 is a broad-spectrum inhibitor with anti-inflammatory activity against multiple targets. Mediators Inflamm 2012: 416036, 2012.
74. Xia ZB, Meng FR, Fang YX, Wu X, Zhang CW, Liu Y, Liu D, Li GQ, Feng FB and Qiu HY: Inhibition of NF-κB signaling pathway induces apoptosis and suppresses proliferation and angiogenesis of human fibroblast-like synovial cells in rheumatoid arthritis. Medicine (Baltimore) 97: e10920, 2018.
75. Zahid A, Li B, Kombe AJK, Jin T and Tao J: Pharmacological inhibitors of the NLRP3 inflammasome. Front Immunol 10: 2538, 2019.